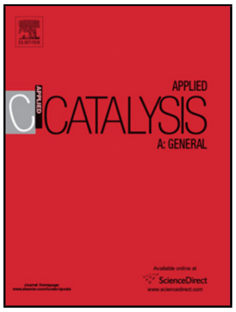

Title: Vapor-phase catalytic dehydration of 2,3-butanediol to 3-buten-2-ol over ZrO_2 modified with alkaline earth metal oxides

Author: Hailing Duan Yasuhiro Yamada Shingo Kubo Satoshi Sato

PII: S0926-860X(16)30561-0
DOI: http://dx.doi.org/doi:10.1016/j.apcata.2016.11.022
Reference: APCATA 16070

To appear in: *Applied Catalysis A: General*

Received date: 7-9-2016
Revised date: 5-11-2016
Accepted date: 15-11-2016

Please cite this article as: Hailing Duan, Yasuhiro Yamada, Shingo Kubo, Satoshi Sato, Vapor-phase catalytic dehydration of 2,3-butanediol to 3-buten-2-ol over ZrO2 modified with alkaline earth metal oxides, Applied Catalysis A, General http://dx.doi.org/10.1016/j.apcata.2016.11.022

A revised manuscript for the original paper submitted to the journal of *Applied Catalysis A*
MS# APCATA-D-16-01586

Vapor-phase catalytic dehydration of 2,3-butanediol to 3-buten-2-ol over ZrO_2 modified with alkaline earth metal oxides

Hailing Duan[a], Yasuhiro Yamada[a], Shingo Kubo[b], Satoshi Sato [a,*]

[a] Graduate School of Engineering, Chiba University, Yayoi, Inage, Chiba 263-8522, Japan
[b] Natural Science Center for Research and Education, Kagoshima University, 1-20-40 Korimoto, Kagoshima, 890-0065, Japan

* Corresponding author. Tel. +81-43-290-3376; fax: +81-43-290-3401
E-mail address: satoshi@faculty.chiba-u.jp (S. Sato)

Graphical abstract

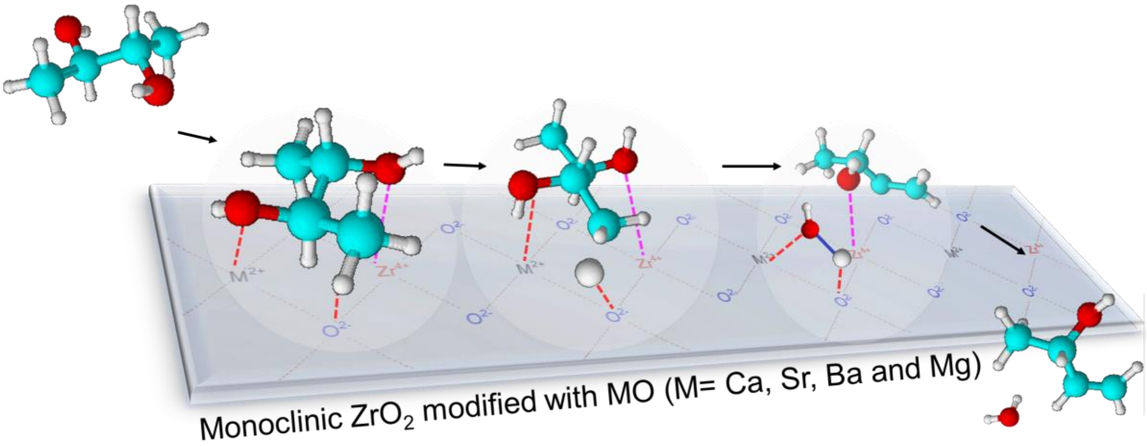

Highlights

- Vapor-phase dehydration of 2,3-butanediol was studied over modified monoclinic ZrO_2.
- 3-Buten-2-ol was preferentially formed over BaO/ZrO_2 and SrO/ZrO_2 as well as CaO/ZrO_2.
- The highest conversion of 72.4% was attained with the selectivity of 74.4% over BaO/ZrO_2.
- XPS study reveals the structure of active sites, M-O-Zr (M= Ca, Sr, and Ba) hetero-linkages.
- The formation of 3-buten-2-ol proceeds via base-acid concerted mechanism.

Abstract

Vapor-phase catalytic dehydration of 2,3-butanediol (2,3-BDO) to produce 3-buten-2-ol (3B2OL) was investigated over several monoclinic ZrO_2 (m-ZrO_2) catalysts modified with alkaline earth metal oxides (MOs), such as SrO, BaO, and MgO, to compare with the previously reported CaO/m-ZrO_2. It was found that those modifiers enhanced the 3B2OL formation to the same level as CaO did by loading an appropriate MO content. Among all the tested catalysts, the BaO/m-ZrO_2 calcined at 800°C with a low BaO content (molar ratio of BaO/ZrO_2 = 0.0452) shows the highest 2,3-BDO conversion (72.4%) and 3B2OL selectivity (74.4%) in the initial stage of 5 h at 350°C. In order to characterize those catalysts, their catalytic activities, crystal structures, and basic properties were studied in detail. In X-ray diffraction (XRD) and X-ray photoelectron spectroscopy (XPS) experiment, it was elucidated that highly dispersed M-O-Zr (M= Ca, Sr, and Ba) hetero-linkages were formed on the surface by loading these MOs onto m-ZrO_2 with an appropriate content and then calcining at 800°C. It can be concluded that the M-O-Zr hetero-linkages generate the proper base-acid balance for the efficient formation of 3B2OL from 2,3-BDO.

Keywords: 2,3-Butanediol; 3-Buten-2-ol; Dehydration; Alkaline earth metal oxides; Monoclinic ZrO_2; Ca-O-Zr hetero-linkage.

1. Introduction

In order to realize the low-carbon society and to diminish the usage of fossil resources, currently, the demand for sustainable chemical compounds is growing rapidly. Among many candidates of sustainable chemical compounds, 2,3-butanediol (2,3-BDO) is one of the potential biomass-derived chemical compounds, and its production has been greatly developed via fermentation with various bacteria from glucose, glycerol, sucrose, and xylose, etc. [1-3] 2,3-BDO shows the future prospect for wide variety of application to biomass-based chemicals via catalytic technologies [4-6]. Studies on 2,3-BDO dehydration were reported even before 1938 [6,7], but the product distribution over different catalysts relies on their acid-base properties, as shown in Scheme 1.

In the dehydration of 2,3-BDO, 2-butanone (MEK) can be produced easily in acidic aqueous solution [8,9], over several acid solid catalysts such as bentonite [7], alumina [10,11], silica-alumina [11], heteropoly acids [12], and zeolites [13-18]. As described in Scheme 1, the hydroxyl group on the 2-position of 2,3-BDO can be easily captured by a proton or an acidic site, and dissociated. Therefore, either hydrogen or methyl group in the 3-position moves to the 2-position as an electron donor, and results in the formation of MEK and 2-metyl-propanal (MPA), respectively (group I in Scheme 1). In the work of Zhang et al., it has been reported that MPA formation competes with MEK formation at a constant ratio of MPA/MEK= ca. 20/68 over HZSM-5 zeolites [16]. In addition, strong acid sites accelerate the migration of methyl group for MPA rather than hydrogen for MEK [17], while alumina and zeolite catalysts are consistently deactivated due to their strong acidity. Nikitina et al. also reported that the presence of Brønsted acid sites in zeolites resulted in the formation of both MEK and MPA, as well as some heavy condensation products, while the Lewis acid sites in alumina act mainly for the MEK formation but with less heavy products. However, when combining the two types of acid sites together, heavy products increased rapidly [18]. It has been also observed that high carbon balance and low coke formation can be obtained via diluting the reactant 2,3-BDO with an appropriate amount of water [10].

1,3-Butadiene (BD) can be also produced from 2,3-BDO together with MEK over acid catalysts such as TiO_2 and γ-Al_2O_3 [10,19]. This is a rare case: both hydroxyl groups of 2,3-BDO must be captured by acid sites, and then dissociated simultaneously or eliminated step by step. Thus, the two terminal hydrogens must also dissociate for the stable BD formation, as shown in groups I and II of Scheme 1.

We have found the direct formation of BD from 2,3-BDO over Sc_2O_3 at high reaction temperatures over 400 ^oC [20], which resembled to ThO_2 as referenced from Winfield's report [21]. However, Sc_2O_3 has weak basic sites without acidic sites [22] while ThO_2 is reported as an acid-base solid [23]. In addition, both of them can yield 3-buten-2-ol

(3B2OL) from 2,3-BDO at low reaction temperatures of 300-350°C [21, 24]. In these cases, 1,2-elimination of a water molecule leads to 3B2OL and then further to BD formation, as shown in group II of Scheme 1. Since the formations of BD and 3B2OL differ in activation energy, their distribution was successfully controlled by reaction temperature.

The 1,2-elimination of 2,3-BDO to produce BD and 3B2OL also occurred over the base-acid bifunctional catalysts such as ZrO_2 [19], CaO/ZrO_2 [25], SiO_2-supported sodium phosphates [26], and SiO_2-supported cesium dihydrogen phosphate [27]. Over the base-acid bifunctional catalysts, the 2-position hydroxyl group of 2,3-BDO was captured by an acid site and dissociated to form a carbon cation, together with the terminal hydrogen by a basic site for a carbon anion. An appropriate base-acid balance is significant for the 1,2-elimination: the excess acid sites result in the formation of MEK, MPA, and the heavy products, while the excess basic sites also lead to the dehydrogenation to produce acetoin and diacetyl [19, 25, 26] or to dehydrate to 2,3-epoxybutane [28], as shown in groups II and III of Scheme 1. On the other hand, supported phosphate catalysts can produce BD at high reaction temperatures but cannot stop the selective formation of 3B2OL [26, 27].

Since the further dehydration of 3B2OL into BD with 94% yield proceeds even at 250°C over Al_2O_3 and SiO_2-Al_2O_3 catalysts [20, 29, 30], 2,3-BDO can be converted into 3B2OL firstly and then further dehydrated into BD by Al_2O_3 at low temperatures. In addition, 3B2OL is also an important chemical compound used as the intermediate for anticancer drugs [31, 32]. In order to synthesize 3B2OL over safe and inexpensive catalysts to take the place of ThO_2 [19] and Sc_2O_3 [20], we have found that the base-acid bifunctional m-ZrO_2 catalysts efficiently work with a basic CaO modifier at a better base-acid balance in the formation of 3B2OL from 2,3-BDO, and speculated the reaction mechanism (Scheme 1 of [25]).

In the present paper, our aim is to prepare more active catalysts than CaO/ZrO_2 for the 3B2OL production from 2,3-BDO. Another aim is to elucidate the active sites of catalyst for the reaction. Thus, we investigated m-ZrO_2 catalysts modified with other MOs such as SrO, BaO, and MgO in the 2,3-BDO dehydration to compare with the results of CaO modifier as reported in the previous work [25]. In addition, XPS of CaO-modified m-ZrO_2 as well as XRD and temperature-programmed desorption (TPD) of CO_2 was performed to further discuss the structure of active sites.

2. Experimental

2.1 *Catalyst preparation*

$Mg(NO_3)_2 6H_2O$, $Ca(NO_3)_2 4H_2O$, $Sr(NO_3)_2$, and $Ba(NO_3)_2$ were purchased from Wako Pure Chemical Industries, Ltd. m-ZrO_2 was supplied as a Japan Reference Catalyst (JRC-ZRO-4) by the Reference Catalyst Division, Catalyst Society of Japan. In the present study, the m-ZrO_2 support was preheated in air at 800 ^oC for 3 h before modification with MOs since m-ZrO_2 calcined at 800 ^oC showed the highest formation rate of 3B2OL from 2,3-BDO [19]. All the MOs were loaded on m-ZrO_2 by incipient wetness impregnation in the same manner as the preparation of CaO/ZrO_2 [25]. The modified ZrO_2 catalysts are expressed as MO-X-T, where M is the loaded alkaline earth metal element, X is the MO loading molar ratio as MO/ZrO_2=X, and T is the calcination temperature (^oC) after impregnation. Additionally, perovskite compounds, $MZrO_3$ with M=Ca, Sr, Ba, and also Mg, were prepared by amorphous citrate process [33] using their nitrates and citric acid with the molar ratio M/Zr/citric acid= 1/1/3 in vacuum at 100^oC for 2 h and then heated at 180^oC for 3 h and finally calcined in air at 800^oC for 3 h.

2.2 *Catalytic reaction*

The catalytic reaction was conducted in a fixed-bed flow reactor under atmospheric pressure of H_2 carrier gas with a flow rate of 80 cm^3 min^{-1} at a temperature of 300-400^oC. After the catalyst (1.0 g) bed had been heated at the prescribed reaction temperature for 1 h, the reactant 2,3-BDO was fed through the reactor top at a liquid feed rate of 11.8 mmol h^{-1}. The liquid effluent was collected hourly at 0^oC and analyzed by gas chromatography (FID-GC-8A, Shimadzu, Japan) with a 60-m capillary column (InertCapWAX-HT). The products were identified by gas chromatography with a mass spectrometer

(GCMS-QP5050A, Shimadzu, Japan) with a 30-m capillary column (DB-WAX). The catalytic activity was evaluated by averaging the conversion and selectivity, defined as mol%, data of the initial 5 h.

2.3 *Characterization*

XRD patterns were measured on New D8 ADVANCE (Bruker) using Cu Kα radiation (λ= 0.154 nm) to detect the catalysts crystal structure. Structural features of CaO/ZrO_2 catalysts were also characterized by XPS (Axis Ultra DLD, Shimadzu Corp.) using X-ray gun of Mg at 10 mA and 10 kV and pass energy of 40 eV. The peak tops of C1s spectra for each samples were 282.8-282.9 eV. The peak top of C1s has been utilized as a reference to adjust binding energies of other orbitals. It indicates that the binding energies of peak tops of other orbitals such as O1s, Ca2p, and Zr3d can be fairly compared. The specific surface area (SA) of catalysts was measured by the Brunauer-Emmett-Teller (BET) theory using the N_2 isotherm at -196◦C. The TPD of adsorbed CO_2 was measured by using a self-made apparatus to estimate the basicity of catalysts [34]. After the sample had been preheated at 500◦C under vacuum, CO_2 was adsorbed at 25^{o}C for 72 h. The temperature of the sample was raised from 25 to 850^{o}C at a temperature-rising rate of 10^{o}C min^{-1}. The amount of desorbed CO_2, which was bubbled into an aqueous solution of NaOH, was monitored by the change in the conductivity of the solution. A cumulative amount of desorbed CO_2 was obtained as a function of the desorbed temperature and then differentiated to give a TPD profile as a basic strength distribution. The amount of basic sites was estimated from the neutralization-titration curves of diluted NaOH. The thermogravimetry-differential thermal analysis (TG-DTA) was performed using Thermoplus 8120E2 (Rigaku, Japan).

3. Results and Discussion

3.1. Catalytic activity of ZrO_2 modified with alkaline earth metal oxides.

The catalytic reaction of 2,3-BDO was investigated over the ZrO_2 modified with MOs such as SrO, BaO, and also MgO at 350°C to compare with the CaO/ZrO_2 catalyst. Figure 1 shows the effects of MO modifier contents on both 2,3-BDO conversion and 3B2OL selectivity. This indicates that the effects of MO modifier contents resembled closely with each other over CaO/ZrO_2, SrO/ZrO_2, BaO/ZrO_2, and MgO/ZrO_2: the 2,3-BDO conversion decreased greatly from ZrO_2 support with increasing their modifier contents, while the 3B2OL selectivity increased greatly only at a small amount of these modifiers and almost unchanged at the large amounts. In the MgO/ZrO_2 catalysts, however, only a low content of MgO could act as a modifier in the similar way to the other MOs for the 3B2OL formation. Besides, the excess MgO inhibits the catalytic activity of ZrO_2: both the 2,3-BDO conversion and the 3B2OL selectivity decreased at the ratio of MgO/ZrO_2 over 0.2. Therefore, due to the high yield of 3B2OL, we choose representative samples with the most proper modifier contents such as CaO-0.0668, SrO-0.0906, BaO-0.0452, and MgO-0.0452 for the further tests.

Figure 2 shows the effects of calcination temperature on the catalytic activities of the modified ZrO_2 catalysts in the dehydration of 2,3-BDO at 350°C. In all the modifiers, especially BaO, the 2,3-BDO conversion was maximized at a calcination temperature of 800°C. In contrast, the 3B2OL selectivity was maintained at high levels and became rarely sensitive to the modifiers when the calcination temperature was higher than 600°C.

In our previous work [25], we investigated the present reaction over the catalysts such as CaO-0.0668-800, SrO-0.0668-800, BaO-0.0668-800, and MgO-0.0668-800 at the same molar MO contents. Among them, CaO-0.0668-800 was the most active catalyst. In the present work, however, it was found that SrO-0.0906-800, BaO-0.0452-800, and MgO-0.0452-800 showed the best catalytic performance in each modified-ZrO_2 series. In addition, BaO-0.0452-800 exceeded CaO-0.0668-800 in the 2,3-BDO conversion.

Figure 3 shows the effect of reaction temperature over the samples of CaO-0.0668-800, SrO-0.0906-800, BaO-0.0452-800, and MgO-0.0452-800, which were calcined at 800°C. The 2,3-BDO conversion increased greatly with increasing the reaction temperature while the highest 3B2OL selectivity was obtained at 350°C. At 350°C, BaO-0.0452-800 showed the same level of 3B2OL selectivity as CaO-0.0668-800 but the highest 2,3-BDO conversion among all the tested catalysts.

In our previous work, it was found that 2,3-BDO conversion decreased slightly in the initial 5 h of time on stream over CaO/ZrO_2 [25] as well as ZrO_2 catalysts [19] while we have not checked their stabilities of catalyst for a long-term operation. Figure 4 shows the catalytic activities of BaO-0.0452-800, CaO-0.0668-800, and m-ZrO_2-800 catalysts for 25 h of time on stream. The m-ZrO_2-800 showed high conversion in the initial stage but deactivated with time on stream. Decline in conversion of BaO-0.0452-800 and CaO-0.0668-800 was also observed in a similar way to that of m-ZrO_2-800. This indicates that the deactivation should be resulted from the support itself. In contrast to the rapid decline of 3B2OL selectivity (from 51.2% to 23.0%) over m-ZrO_2-800, the 3B2OL selectivity decreased gradually over BaO-0.0452-800 and CaO-0.0668-800 (from ca. 75% to ca. 60%). It depicts that the MO modifiers enhanced not only the 3B2OL selectivity but also the alleviation for the catalytic deactivation. In addition, contrary to the decline of the 3B2OL selectivity, the byproducts such as MEK, acetoin, MPA, and 2-methyl-propanol increased. After 25 h of time on stream over m-ZrO_2-800, the selectivities of MEK, acetoin, and MPA increased from the initial 20.2, 4.9, and 5.4% to 35.5, 22.1, and 12.4%, respectively. In contrast, the selectivities of MEK, acetoin, and MPA over BaO-0.0452-800 increased from 6.6, 3.4, and 3.3% to 11.7, 16.3, and 3.4%, respectively. This indicates that BaO-0.0452-800 increases dehydrogenation ability to form acetoin during the gradual deactivation. The reasons of catalytic deactivation are not clear: no clear changes were observed in their crystal structures from the XRD patterns of these catalysts before and after the reaction for 25 h. Besides, the deposited coke was observed less than 1.5 wt.% over the modified ZrO_2 and m-ZrO_2-800 after being used for 25 h (TG-DTA data not shown). Thus, coke should not be the main reason for deactivation.

In the ZrO_2 modified with an appropriate content of MOs such as CaO, SrO, BaO, and also MgO, the catalytic activities of m-ZrO_2 were enhanced efficiently for the 3B2OL formation. Their catalytic activities resembled closely with each other for their loaded contents, calcination temperatures, reaction temperatures, and also stabilities with time on stream (Figures 1-4). In addition, among the four modified catalysts, SrO/ZrO_2 and BaO/ZrO_2 also acted well for both 2,3-BDO conversion and 3B2OL selectivity while those of MgO/ZrO_2 were always the lowest. In the following sections, in order to identify the key factors for the enhancement of the present reaction, their structural and basic properties were investigated.

3.2. Structural properties of ZrO_2 modified with alkaline earth metal oxides.

Figure 5 shows XRD patterns of the typical samples with different calcination temperatures and MO contents. In the samples, main diffraction peaks are attributed from m-ZrO_2 with several additional peaks of perovskite compounds such as $CaZrO_3$, $SrZrO_3$, and $BaZrO_3$. High MO contents and high calcination temperatures induced the formation of the new perovskite phases. In addition, both the formation and the crystalline growth of these new perovskite phases can be also observed in the order of $BaZrO_3 > SrZrO_3 > CaZrO_3$. In contrast to $CaZrO_3$, $BaZrO_3$, and $SrZrO_3$ phases were detected even at low MO contents and low calcination temperatures < 800°C. However, in MgO/ZrO_2 samples, no peaks assigned to $MgZrO_3$ were detected, while the crystalline of m-ZrO_2 phase grew obviously with increasing both MgO content and calcination temperature. Thus, it is reasonable that the 3B2OL selectivity was enhanced over MgO/ZrO_2 due to the crystalline growth of m-ZrO_2, which is the most efficient ZrO_2 crystal phase for the 3B2OL formation, as described in our previous work [19]. Here, we have to check the catalytic activity of perovskite compounds such as $CaZrO_3$, $SrZrO_3$, and $BaZrO_3$.

In order to investigate the catalytic activities of the perovskite compounds, we prepared $CaZrO_3$, $SrZrO_3$, and $BaZrO_3$. As listed in Table 1, we succeeded in preparing these perovskite compounds (XRD patterns in Figure 5b) but even together with a small amount of $SrCO_3$ and $BaCO_3$, which are difficult to be removed during the preparation and characterization processes in air. The results in the catalytic reaction emphasized that all the perovskite compounds showed no catalytic activity for the formation of 3B2OL from

2,3-BDO: not only the extremely low 2,3-BDO conversion but also the low 3B2OL selectivity were obtained. It can be understood that these perovskite compounds such as $CaZrO_3$, $SrZrO_3$, and $BaZrO_3$ detected in the modified m-ZrO_2 could not provide the active sites for the 3B2OL production.

Figure 6 shows the O1s, Ca2p, and Zr3d XPS spectra of CaO-0.0668-800, CaO-0.226-800, and CaO-0.0668-600 samples together with CaO-800, ZrO_2-800, and $CaZrO_3$-800. Firstly, from the O1s spectra of the samples, the peak position at 527.45 eV, which is different from those of both CaO-800 (529.45 eV) and ZrO_2-800 (527.83 eV), was found to be the same as that from $CaZrO_3$-800. In our previous work, Ca-O-Zr hetero-linkages are also confirmed by the DRIFT spectra of CaO-X-800 samples [25]. Thus, the new peak at 527.45 eV should be assigned to the O1s peak of Ca-O-Zr hetero-linkages, which would attribute to the base structure of $CaZrO_3$. The results also well agree with some other works [35-42]. In addition, the XPS spectra of Ca2p and Zr3d also support the Ca-O-Zr hetero-linkage formation: $Ca2p_{1/2}$ shifted from 344.92 to 344.31 eV and that of $Ca2p_{3/2}$ from 348.55 to 348.03 eV, together with $Zr3d_{3/2}$ shifting from 182.26 to 181.81 eV and that of $Zr3d_{5/2}$ from 179.92 to 179.47 eV. On the other hand, among the CaO/ZrO_2 samples, CaO-0.0668-800 presents the highest percentage of Ca-O-Zr state via its O1s XPS spectra, as well as the spectra of Ca2p and Zr3d. However, in comparison with CaO-0.0668-800, the spectra of CaO-0.226-800 show lower percentages of Ca-O-Zr hetero-linkages, but this contradicts with their XRD patterns (Figure 5a), in which stronger peaks assigned to $CaZrO_3$ phase were detected in CaO-0.226-800 rather than CaO-0.0668-800. This indicates that, unlike CaO-0.226-800, Ca-O-Zr hetero-linkages are highly dispersed on the surface of CaO-0.0668-800 at the appropriate CaO loading. In CaO-0.226-800 with excess CaO content, most Ca-O-Zr hetero-linkages are gathered to form $CaZrO_3$ crystal phase, which is not active for the formation of 3B2OL from 2,3-BDO (Table 1). At a low calcination temperature of 600 ^{o}C, however, no proof of the Ca-O-Zr hetero-linkage can be found from the CaO-0.0668-600 sample in its O1s, Ca2p or Zr3d XPS spectra. In addition, the XRD pattern of CaO-0.0668-600 sample (Figure 5a), as well as the samples calcined at lower than 800^{o}C in our previous work [25], displayed no peaks assigned to $CaZrO_3$ phase. It indicates that high calcination temperature at 800^{o}C or higher is needed for the formation of Ca-O-Zr hetero-linkage and then for $CaZrO_3$ phase. Furthermore, some groups also reported that they succeeded in preparing $CaZrO_3$ at high temperatures over 800^{o}C [37-41].

Figure 7 shows TG-DTA profiles of the alkaline earth metal nitrate loaded on m-ZrO_2 samples prior to calcination. These alkaline earth metal nitrates have different difficulties in decomposing with increasing calcination temperature, and the difficulty increases in the order of $Mg(NO_3)_2 < Ca(NO_3)_2 < Sr(NO_3)_2 < Ba(NO_3)_2$. The decomposition has almost finished at lower than 600^{o}C (Figure 7a). The results are also well accordance with the O1s XPS spectra shown in Figure 6, in which only the O1s XPS peaks attributed to CaO and ZrO_2 were detected from CaO-0.0668-600 sample and no O1s XPS peak attributed to $Ca(NO_3)_2$ were observed. It is reasonable that these alkaline earth metal nitrate decomposed at temperatures lower than 600^{o}C for the formation of CaO, and then Ca^{2+} of CaO immerged into ZrO_2 to form Ca-O-Zr hetero-linkage at around 800^{o}C, and that more Ca-O-Zr hetero-linkages gathered and transformed to $CaZrO_3$ phase at calcination temperatures higher than 800^{o}C. Judging from the XRD patterns, it is reasonable that the formation of M-O-Zr hetero-linkage and the transformation to perovskite phases over SrO/ZrO_2 and BaO/ZrO_2 samples should have occurred at lower temperatures than that of CaO/ZrO_2. However, their weight losses continued above 600^{o}C even with a small amount, especially the BaO-0.0452 sample seems to be further decomposed at higher than 1000^{o}C (Figure 7b). The weight loss after 600^{o}C should be attributed to the decomposition of their carbonates, which form easily in air environment containing CO_2.

3.3 Basic properties of ZrO_2 modified with alkaline earth metal oxides.

In our previous paper, the basic properties of CaO/ZrO_2 have been reported in detail [25]. Figure 8 shows the basic properties of MgO/ZrO_2, SrO/ZrO_2, and BaO/ZrO_2 investigated by CO_2-TPD. Among the samples, the CO_2 desorption peaks attributed to weak basic sites were detected as shifting slightly from 77°C to 115°C (peaks α and α'), and their amount increased properly with increasing the MO contents. Besides, the desorption peak β attributed to new medium basic sites was also found at around 350°C from SrO/ZrO_2 and BaO/ZrO_2 in the same way as CaO/ZrO_2 [25]. The peaks γ at temperatures higher than 600°C were detected over SrO/ZrO_2 and BaO/ZrO_2 which could be resulted from the CO_2 desorbed from the isolated SrO and BaO. The peaks higher than 800°C could be resulted from the decomposition of their carbonates. In the actual reactions performed at 350 °C, the peak γ of the adsorption sites, which strongly adsorb CO_2, could not be attributed to the reaction.

On the other hand, new peaks generated on MgO/ZrO_2 samples were detected at around 250°C, such changes on its basic property must be related to the structural changes as described in the previous section of XRD (Figure 5a). The desorption peaks at 335°C are resulted from the excess MgO and it should be the reason for the decrease in the catalytic activity of MgO/ZrO_2 catalysts in Figure 1. The CO_2-TPD profiles of MgO/ZrO_2 resemble closely to the reports elsewhere [43-45].

The intensity of peak β varies with increasing the MO contents. Especially, at molar ratio $MgO/ZrO_2 = 0.0226$, $SrO/ZrO_2 = 0.0906$, and $BaO/ZrO_2 = 0.0452$ as well as $CaO/ZrO_2 = 0.0668$ in the previous report [25], the largest amount of basic sites β were detected. The samples calcined at 800°C show the largest amount of basic sites β, but the amount decreased with increasing calcination temperature. Of course, the catalysts with the largest amount of basic sites β were also confirmed as the most active ones for high 2,3-BDO conversion and high 3B2OL selectivity. The results are also well accordance with the report of CaO/ZrO_2 catalysts [25].

Figure 9 shows CO_2-TPD profiles of the perovskite compounds of $MZrO_3$ (M= Ca, Sr, and Ba), which showed no good catalytic activities for the 3B2OL formation from 2,3-BDO, together with the MgO-ZrO_2 composed of tetragonal ZrO_2 (Table 1). Over the perovskite compounds of $MZrO_3$, the decomposition peaks resulted from their carbonates were mainly observed but rare basic sites appeared. Over the MgO-ZrO_2 i.e. tetragonal ZrO_2, large desorption peaks attributed to new basic sites with medium strength were observed at around 250ºC. As reported in our previous work [19, 25], tetragonal ZrO_2 was not suitable for the formation of BD and 3B2OL from 2,3-BDO. In the present study, however, the new medium-strength basic sites would have contributed to the formation of 3B2OL even with a low reactant conversion.

Although the perovskite compounds of $MZrO_3$ have no active basic sites β, $MZrO_3$ phase was detected in the XRD patterns of modified m-ZrO_2 catalysts which showed catalytic activities for the present reaction. However, among the CaO/ZrO_2 catalysts, CaO-0.0668-800 has only weak XRD peaks attributed to $CaZrO_3$, but it has the most percentages of O1s XPS peak assigned to the Ca-O-Zr hetero-linkages highly dispersed on its surface. The hetero-linkages could attribute to the most amount of basic sites β, and also enhance the 3B2OL formation from 2,3-BDO. As discussed in the research of Zhang's group [46], the uneven distribution in charges of the Ca-O-Zr hetero-linkage generates new acidic and basic sites, which is different from those of the pure CaO and ZrO_2. In the XPS spectra of the samples containing Ca-O-Zr hetero-linkage (Figure 6), it was found that not only the O1s, but also their Ca2p and Zr3d spectra shifted to lower energy positions as compared with those of pure CaO and ZrO_2. Thus, the bond distances of Ca-O-Zr should be different from those of pure CaO and ZrO_2. Since we found that the formation rate of some unsaturated alcohols from diols are sensitive to the ionic radii of cations in the rare earth metal oxide catalysts [6,24], the distance between these active sites imaged as our work [25] should also be adjusted suitably by the highly dispersed hetero-linkages for the present reaction. In addition, the O1s spectra shifting to lower energy positions would contribute to the new medium basic sites β, which we speculated as the O^{2-} from Ca-O-Zr hetero-linkage. Since the O^{2-} of CaO has stronger base than that of ZrO_2, the O^{2-} from Ca-O-Zr results in weaker medium basic sites β than the O^{2-} of CaO, but still stronger than that of ZrO_2. On the other hand, their Ca2p and Zr3d spectra shifting to lower energy positions must also adjust the acidic sites balance which should be much more suitable for the present reaction. We have proposed that the formation of 3-buten-2-ol proceeds via base-acid concerted mechanism (Scheme 1 of [25]). The present MO/m-ZrO_2 catalysts must efficiently work with the basic modifiers in a fine base-acid balance for the formation of 3B2OL from 2,3-BDO. Since Zhang groups detected the changes in acidity of CaO/ZrO_2 via NH_3-TPD [46], we will perform further work to identify these acid sites of the modified ZrO_2 catalysts.

4. Conclusions

Vapor-phase catalytic dehydration of 2,3-BDO to 3B2OL was investigated over several modified m-ZrO_2 catalysts such as MgO/m-ZrO_2, SrO/m-ZrO_2, and BaO/m-ZrO_2 to compare with the previously reported CaO/m-ZrO_2. In the dehydration of 2,3-BDO, it was found that 3-buten-2-ol was preferentially formed over BaO/ZrO_2 and SrO/ZrO_2 as well as CaO/ZrO_2. Especially, BaO-0.0452-800 showed the highest 2,3-BDO conversion of 72.4% and the 3B2OL selectivity of 74.4% in the initial stage of 5 h at 350^{o}C. However, all these catalysts declined the catalytic activity in a long-term operation of 25 h. Compared with the rapid decline of 3B2OL formation over m-ZrO_2-800 support, the decline over m-ZrO_2 modified with alkaline earth metal oxides, BaO-0.0452-800 and CaO-0.0668, was gradual.

XRD and XPS studies elucidated the active structure of modified ZrO_2 catalysts. M-O-Zr (M= Ca, Sr, and Ba) hetero-linkages were highly dispersed on the surface by loading these MOs onto m-ZrO_2 with an appropriate content and then calcining at 800^{o}C. Perovskite compounds such as $CaZrO_3$, which was newly produced in the catalysts, was inactive for the reaction. It can be concluded that the highly dispersed M-O-Zr (M= Ca, Sr, and Ba) hetero-linkages on the surface is formed to adjust the appropriate distance of these active sites and also to generate the proper base-acid balance for the efficient formation of 3B2OL from 2,3-BDO.

Acknowledgements

This research was partly supported by JST, Strategic International Collaborative Research Program, SICORP.

References

[1] S. Lee, B. Kim, K. Park, Y. Um, J. Lee, Appl. Biochem. Biotechnol. 166 (2012) 1801-1813.

[2] X. Ji, H. Huang, P. Ouyang, Biotechnol. Adv. 29 (2011) 351-364.

[3] A. Zeng, W.Sabra, Curr. Opin. Biotechnol. 22 (2011) 749-757.

[4] P. Lanzafame, G. Centi, S. Perathoner, Chem. Soc. Rev. 43 (2014) 7561-7580.

[5] E.V. Makshina, M. Dusselier, W. Janssens, J. Degre’ve, P.A. Jacobs, B.F. Sels, Chem. Soc. Rev. 43 (2014) 7917-7953.

[6] H. Duan, Y. Yamada, S. Sato, Chem. Lett. 45 (2016) 1036-1047.

[7] A.N. Bouns, R.V.V. Nicholls, Can. J. Res. 25B (1947) 80-89.

[8] R.R. Emerson, M.C. Flickinger, G.T. Tsao, Ind. Eng. Chem. Prod. Res. Dev. 21 (1982) 473-477.

[9] A.C. Neish, V.C. Haskell, F.J. MacDonald, Can. J. Res. 23B (1945) 281-289.

[10] X. Liu, V. Fabos, S. Taylor, D.W. Knight, K. Whiston; G.J. Hutchings, Chem. Eur. J. 22 (2016) 12290-12294.

[11] A.V. Tran, R.P. Chambers, Biotechnol. Bioeng. 29 (1987) 343-351.

[12] B. Török, I. Pálinkó, Á. Molnár, M. Rózsa-Tarjáni, J. Mol. Struct. 482–483 (1999) 329-332.

[13] M.A. Nikitina, V.L. Sushkevich, I.I. Ivanova, Petrol. Chem. 56 (2016) 230-236.

[14] C.P. Bezouhanova, F.A. Jabur, J. Mol. Catal. 87 (1994) 39-46.

[15] A. Multer, N. McGraw, K. Hohn, P. Vadlani, Ind. Eng. Chem. Res. 52 (2013) 56-60.

[16] W. Zhang, D. Yu, X. Jia, H. Huang, Green Chem. 14 (2012) 3441-3450.

[17] J. Zhao, D. Yu, W. Zhang, Y. Hu, T. Jiang, J. Fu, H. Huang, RSC Adv. 6 (2016) 16988-16995.

[18] M.A. Nikitina, I.I. Ivanova, ChemCatChem. 8 (2016) 1346-1353.

[19] H. Duan, D. Sun, Y. Yamada, S. Sato, Catal. Commun. 48 (2014) 1-4.

[20] H. Duan, Y. Yamada, S. Sato, Appl. Catal. A: Gen. 491 (2015) 163-169.

[21] M.E. Winfield, J. Council Sci. Ind. Res. 18 (1945) 412-423.

[22] S. Sato, R. Takahashi, M. Kobune, H. Gotoh, Appl. Catal. A: Gen. 356 (2009) 57-63.

[23] A. Auroux, A. Gervasini, J. Phys. Chem. 94 (1990) 6371-6379.

[24] H. Duan, Y. Yamada, S. Sato, Chem. Lett. 43 (2014) 1773-1775.

[25] H. Duan, Y. Yamada, S. Sato, Appl. Catal. A: Gen. 487 (2014) 226-233.

[26] W. Kim, W. Shin, K. Lee, H. Song, H. Kim, D. Seung, I. Filimonov, Appl. Catal. A: Gen. 511 (2016) 156-167.

[27] D. Tsukamoto, S. Sakami, M. Ito, K. Yamada, T. Yonehara, Chem. Lett. 45 (2016) 831-833.

[28] T. Kim, J. Baek, C. Song, Y. Yun, D. Park, W. Kim, J. Han, J. Yi, J. Catal. 323 (2015) 85-99.

[29] N. Ichikawa, S. Sato, R. Takahashi, T. Sodesawa, J. Mol. Catal. A: Chem. 256 (2006) 106-112.

[30] E.V. Makshina, M. Dusselier, W. Janssens, J. Degre`ve, P.A. Jacobsa, B.F. Sels, Chem. Soc. Rev. 43 (2014) 7917-7953.

[31] J.W. Bode, E.M. Carreira, J. Org. Chem. 66 (2001) 6410-6424.

[32] J.W. Bode, E.M. Carreira, J. Am. Chem. Soc. 123 (2001) 3611-3612.

[33] D.J. Anderton, F.R. Sale, Powder Metallurgy 22 (1979) 14-21.

[34] S. Sato, K. Koizumi, F. Nozaki, J. Catal. 178 (1998) 264-274.

[35] R. Koirala, K.R. Gunugunuri, S.E. Pratsinis, P.G. Smirniotis, J. Phys. Chem. C 115 (2011) 24804-24812.

[36] H. Guo, S. Wang, C. Li, Y. Zhao, Q. Sun, X. Ma, Ind. Eng. Chem. Res. 55 (2016) 7873-7879.

[37] G. Cabello, L. Lillo, C. Caro, G.E. Buono-Core, B. Chornik, M. Flores, C. Carrasco, C.A. Rodriguezd, Ceram.Int. 40 (2014) 7761-7768.

[38] X.Y. Qiu, H. W. Liu, F. Fang, M.J. Ha, X.H. Zhou, J.M. Liu, Appl. Phys. A 81 (2005) 1431-1434.

[39] H. Wang, S. Liu, W. Zhang, N. Zhao, W. Wei, Y. Sun, Acta Chim. Sinica 64 (2006) 2409-2413.

[40] A.Y. Teterin, K.I. Maslakov, Y.A. Teterin, K.E. Ivanov, S.V. Yudintsev, S.V. Stefanovsky, T.S. Livshits, M.I. Lapina, Nucl. Technol. Radiat. 25 (2010) 157-163.

[41] J. Chen, S. Wu, F. Zhang, S. Lü, Y. Mao, Mater. Chem. Phys. 172 (2016) 87-97

[42] S. Yan, M. Kim, S. Mohan, S.O. Salley, K.Y. Simon Ng, Appl. Catal. A: Gen. 373 (2010) 104-111.

[43] Y. Yanagisawa, K. Takaoka, S. Yamabe, T. Ito, J. Phys. Chem. 99 (1995) 3704-3710.

[44] J.I. Di Cosimo, V.K. Díez, C. Ferretti, C.R. Apesteguía, Catalysis 26 (2014) 1-28.

[45] S. Liu, X. Zhang, J. Li, N. Zhao, W. Wei, Y. Sun, Catal. Commun. 9 (2008) 1527-1532.

[46] Q. Zhang, Y. Zhang, H. Li, C. Gao, Y. Zhao, Appl. Catal. A: Gen. 466 (2013) 233-239.

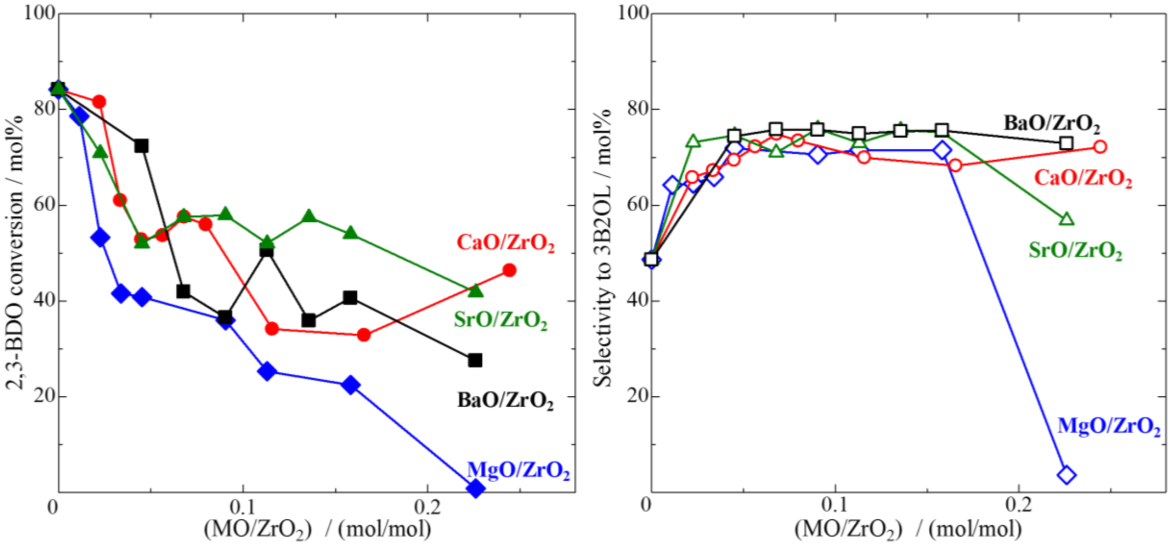

Figure 1 Effects of alkaline earth metal oxide contents on the catalytic activities of modified ZrO_2 catalysts in the dehydration of 2,3-BDO to 3B2OL at 350°C. All the catalysts were calcined at 800°C.

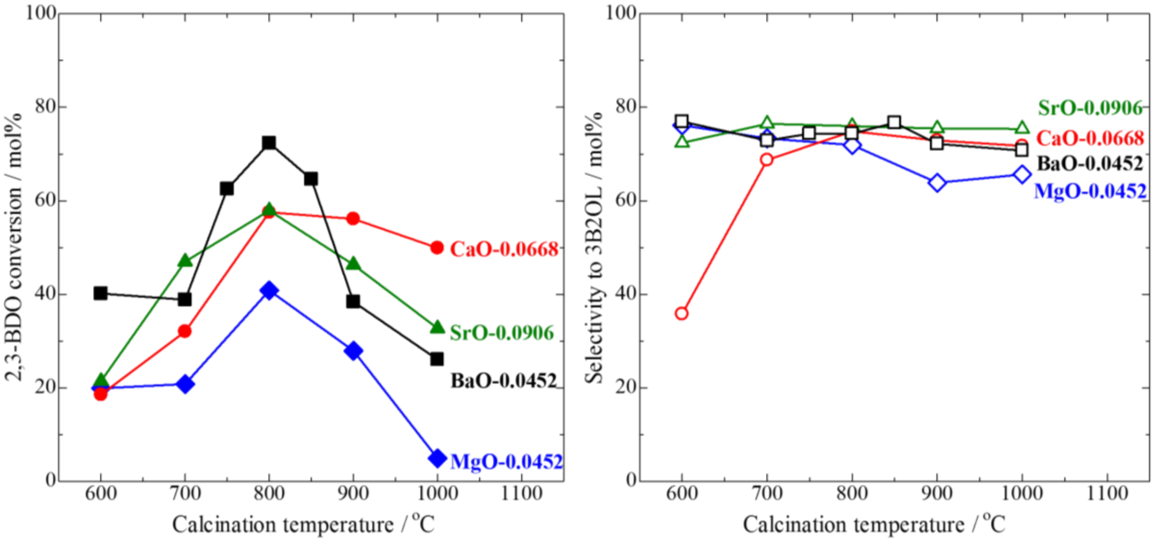

Figure 2 Effects of calcination temperature on the catalytic activities of modified ZrO_2 catalysts in the dehydration of 2,3-BDO to 3B2OL at 350°C.

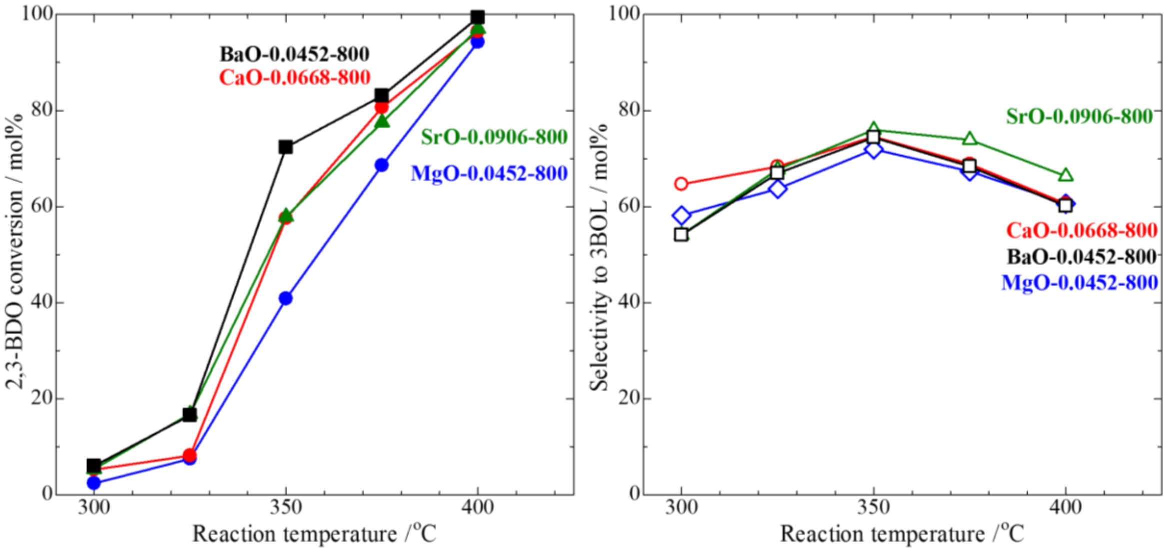

Figure 3 The catalytic activities of modified ZrO_2 catalysts in the dehydration of 2,3-BDO to 3B2OL as a function of reaction temperature.

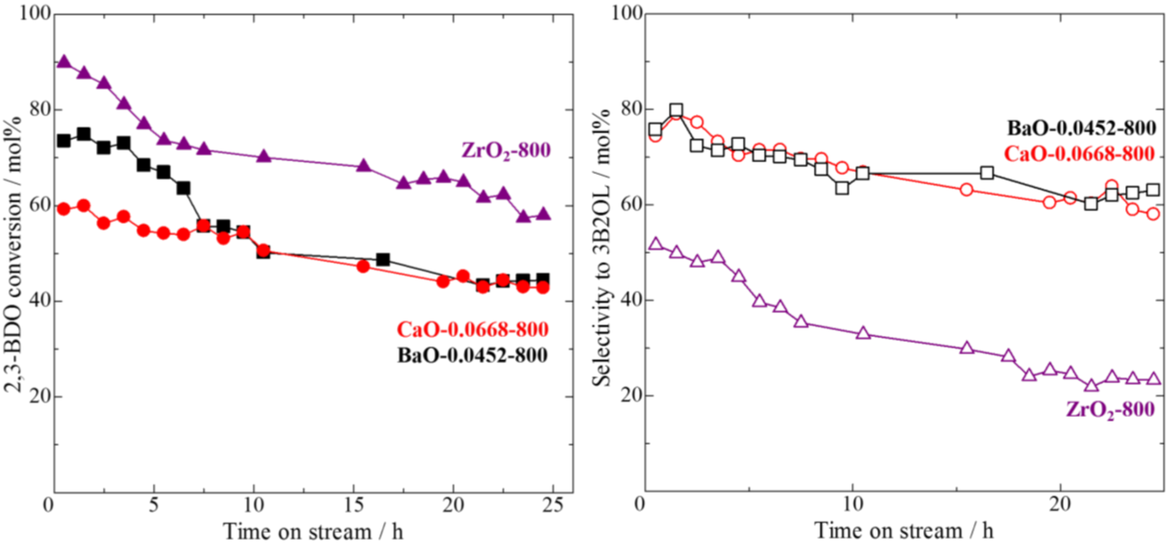

Figure 4 Catalytic stability of modified ZrO_2 catalysts with time on stream at 350°C.

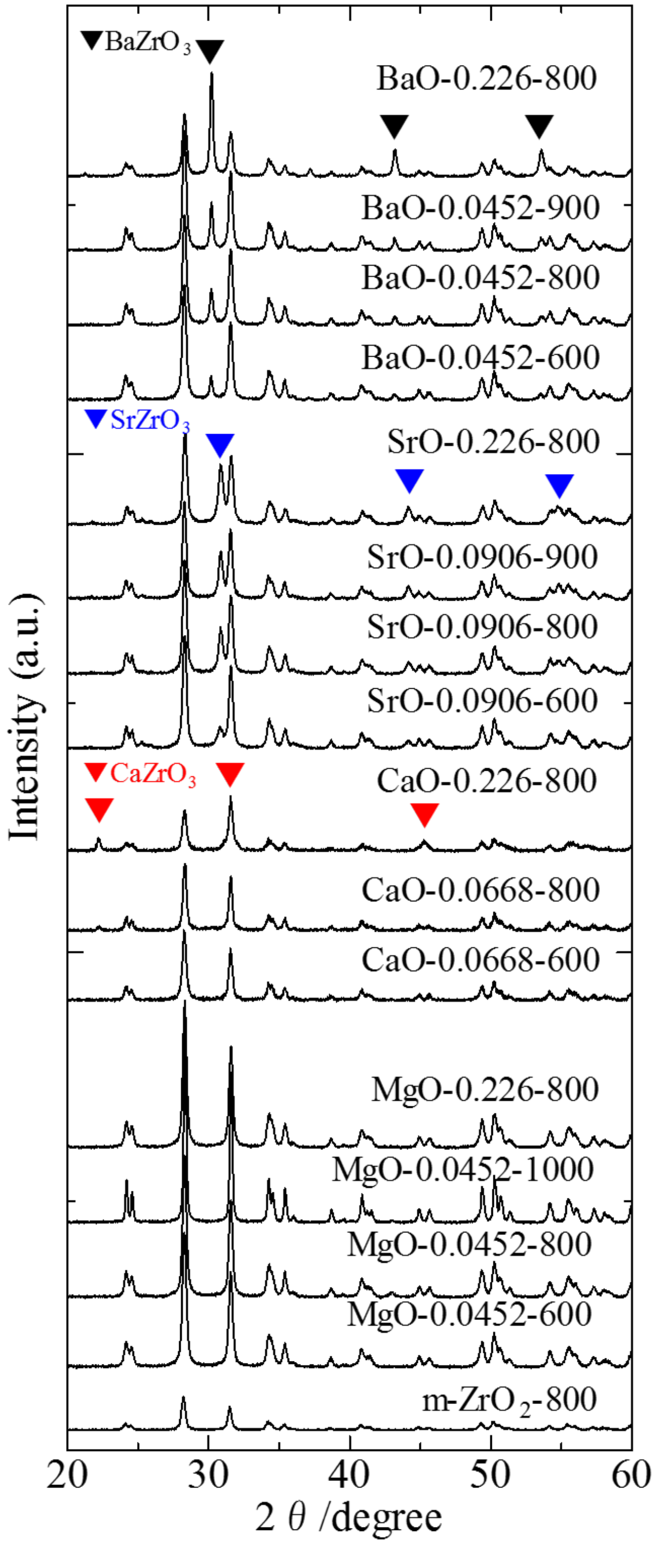

Figure 5 (a) XRD patterns of modified ZrO_2 catalysts: effects of calcination temperature and the alkaline earth metal oxide contents on their crystal structures.

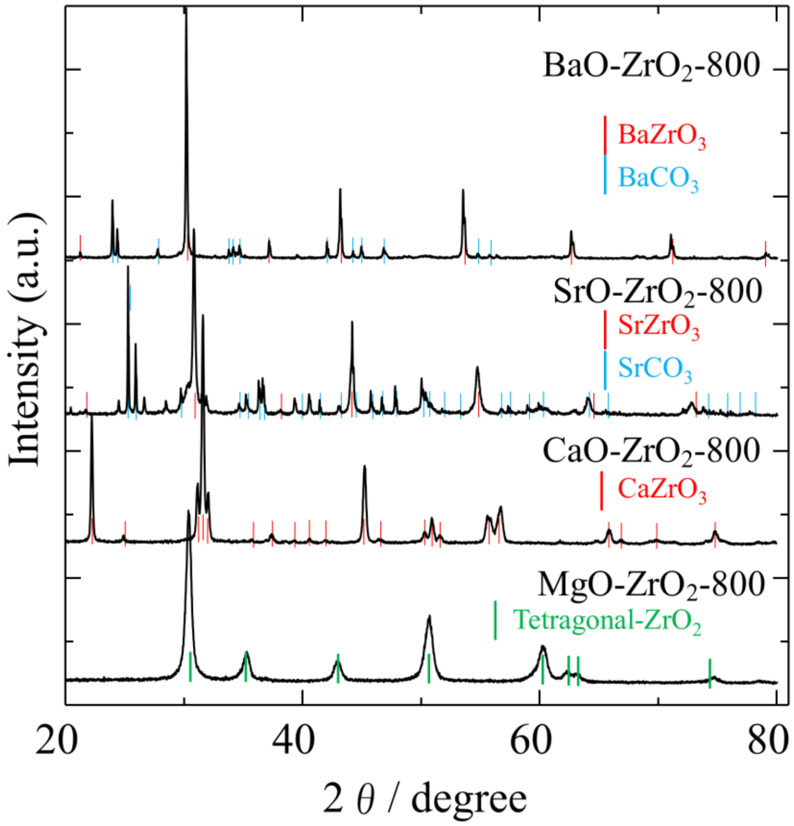

Figure 5 (b) XRD patterns of perovskite compounds ($MZrO_3$) aimed samples: the names in black are their aimed compositions, and the terms in red and blue are the phases detected from these samples.

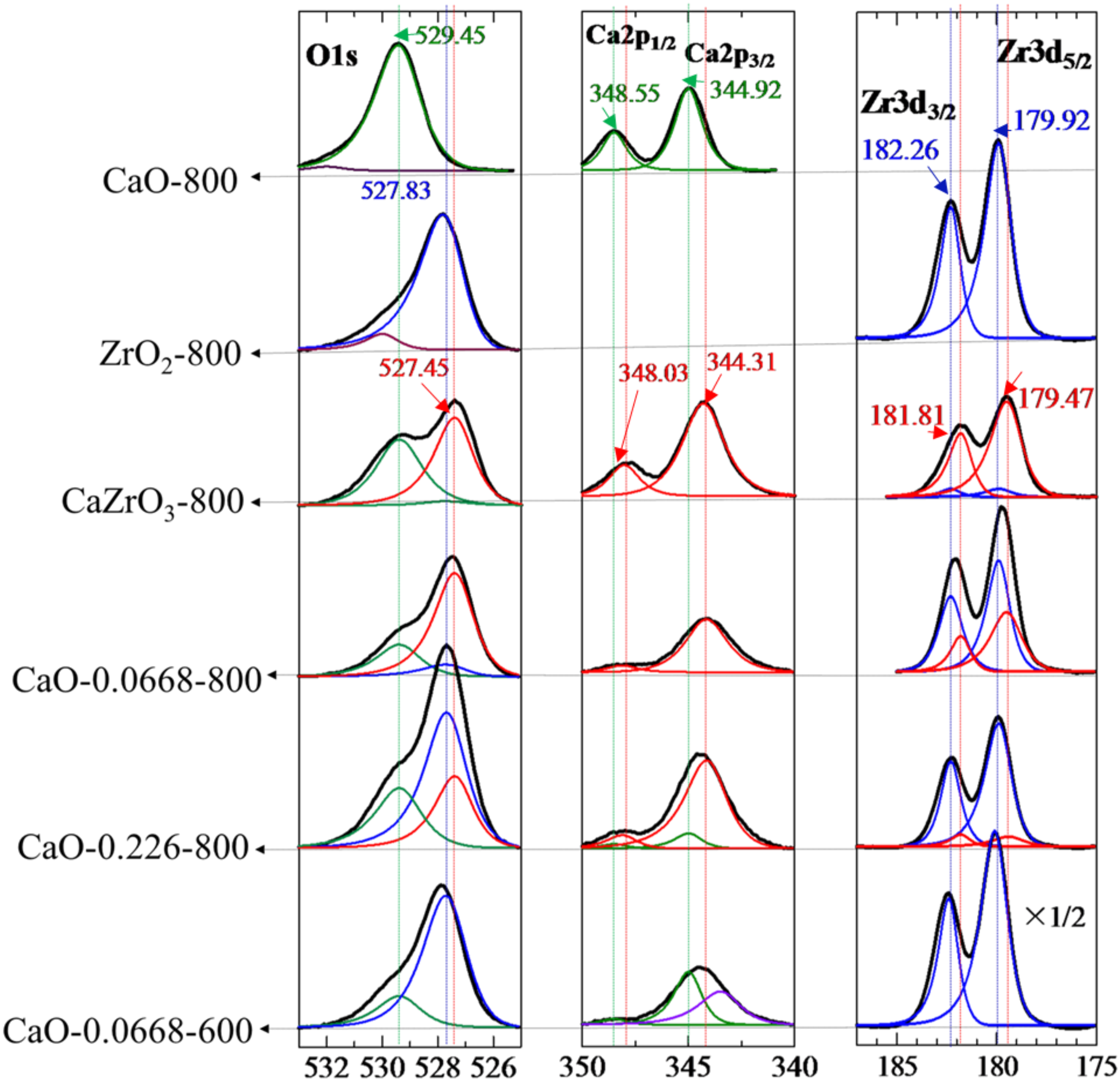

Figure 6 O1s, Ca2p, and Zr3d XPS spectra of CaO-800, ZrO_2-800, $CaZrO_3$-800, CaO-0.0668-800, CaO-0.226-800, and CaO-0.0668-600.

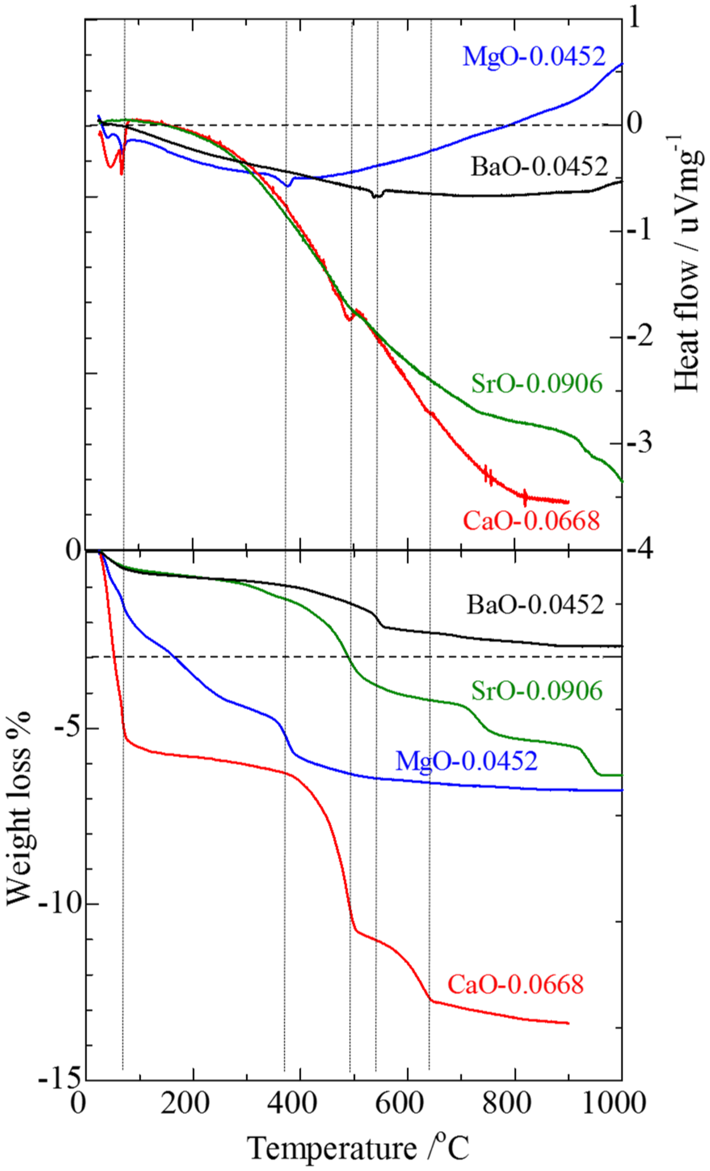

Figure 7 TG-DTA profiles of the alkaline earth metal nitrate loaded on m-ZrO_2 samples.

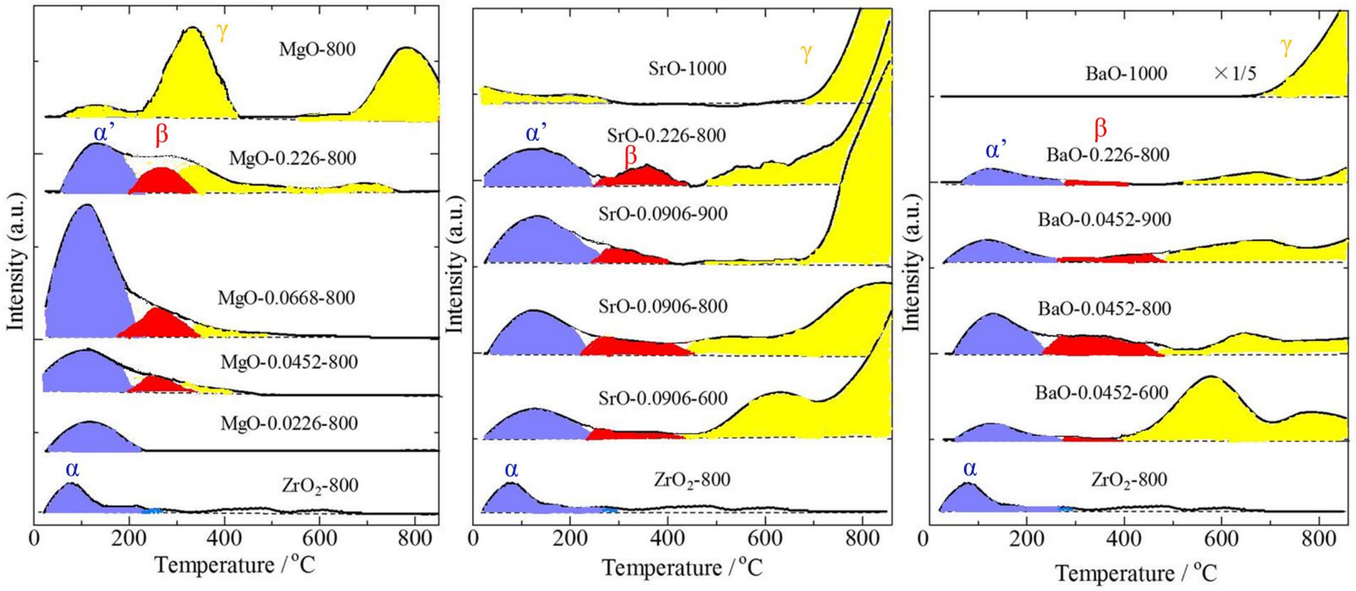

Figure 8 Effects of calcination temperature and alkaline earth metal oxide contents on the basic properties (CO_2-TPD) of the modified catalysts.

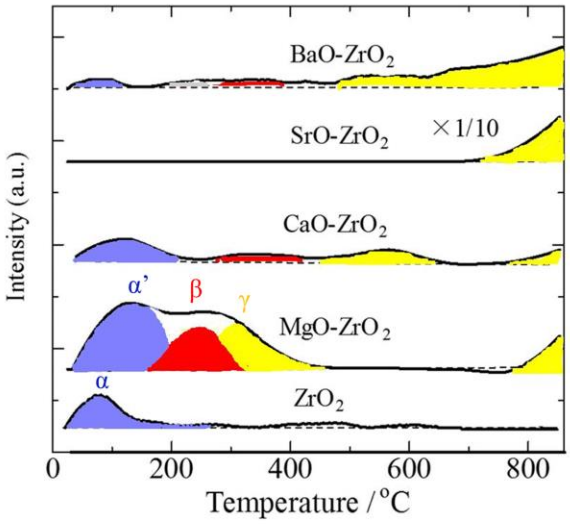

Figure 9 CO_2-TPD profiles of the perovskite compounds shown in Fig. 5(b), MgO-ZrO_2 and m-ZrO_2.

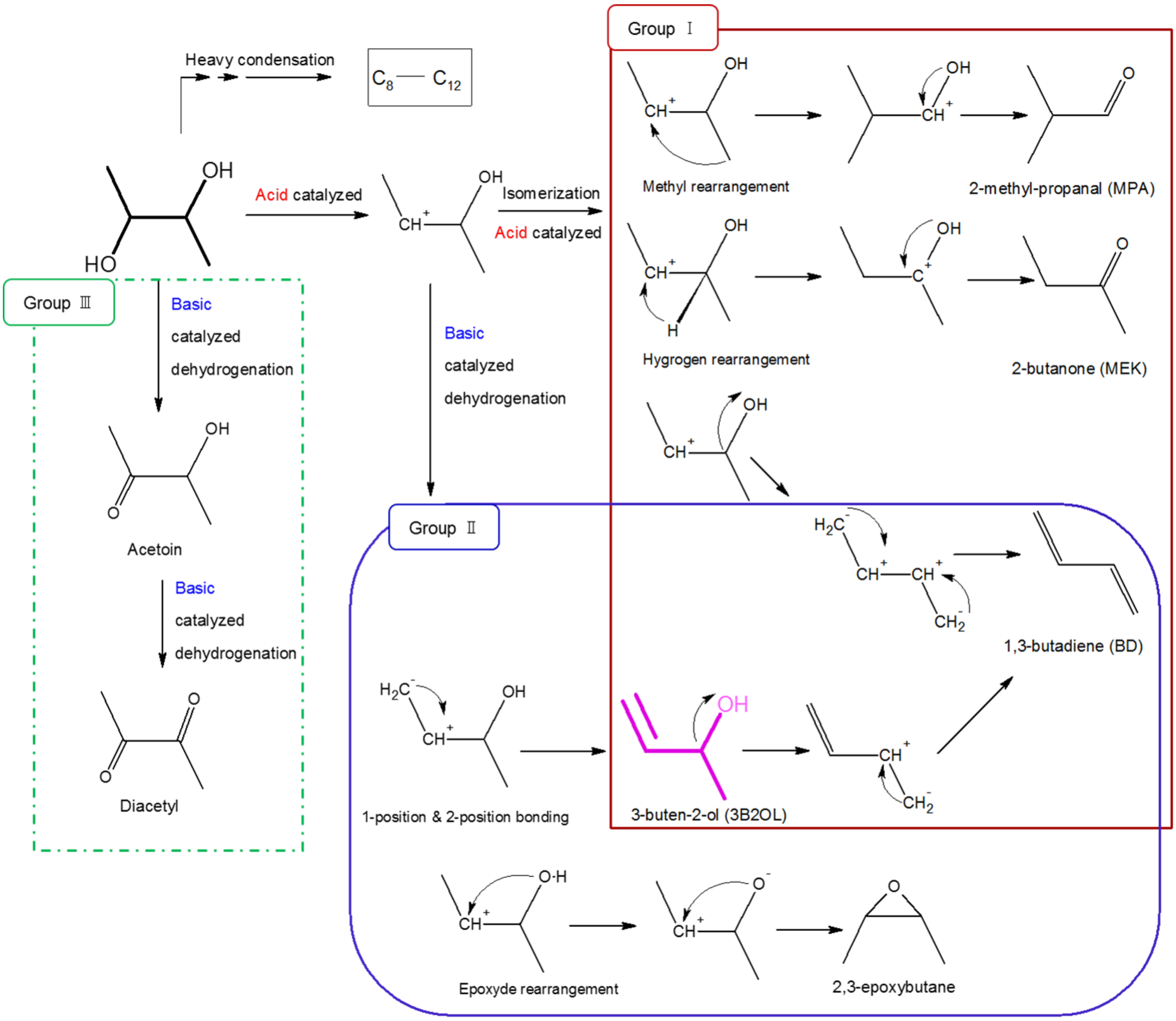

Scheme 1 Possible chemical compounds from 2,3-BDO catalyzed by acid and base catalysts.

Table 1 Reaction activities of perovskite compounds ($MZrO_3$), MgO-ZrO_2 and m-ZrO_2 in the dehydration of 2,3-butanediol at 350°C.

Catalyst	S.A.	Crystal phase	Conversion	Selectivity (mol%)			
(1.0 g)	(m^2 g^{-1})		(mol%)	3B2OL	MEK	Acetoin	Others
Blank test			1.7	7.5	12.9	47.2	32.4
MgO-ZrO_2	16.5	Tetragonal ZrO_2	16.4	52.6	9.4	20.6	17.4
CaO-ZrO_2	7.4	$CaZrO_3$	4.5	0	11.8	64.9	23.3
SrO-ZrO_2	< 1	$SrZrO_3$+$SrCO_3$	3.3	7.1	11.0	76.0	5.9
BaO-ZrO_2	< 1	$BaZrO_3$+$BaCO_3$	0.9	5.9	13.6	69.8	10.7
m-ZrO_2	26.3	Monoclinic ZrO_2	97.6	43.9	22.7	1.7	31.8

All the catalysts were calcined at 800°C during the preparation procedure.